자작 전기차의 프레임 구조 안전을 위한 개선 설계

Improved Design for Frame Structure Safety in Self-Made Electric Vehicles

한민웅, *황승언, #문현호, 이종선
한동대학교 기계제어공학부
Min-woong Han, *Seung-eun Hwang, #, Hyeon-ho Moon, and Chong-sun Lee
School of mechanical and control engineering, Handong Global University

ABSTRACT
Our study utilized ANSYS software for achieving stable high-speed performance in a custom electric vehicle competition. The primary focus was on addressing the challenges posed by chain drive tension in high-speed electric vehicle design. This tension leads to two main issues: rotational instability in the motor case, fixed at two points, causing unwanted chain slack, and excessive stress beneath the LSD and motor case frames, surpassing yield limits. Our objective was to systematically analyze and mitigate these issues to enhance vehicle performance and reliability. We calculated maximum chain tension under extreme conditions, established realistic boundary conditions, and conducted simulations to evaluate stress and displacement during real driving scenarios. Considering the chain's cyclic loading during regular operation, a zero-based force fatigue analysis was essential for ensuring the structural integrity of key components. In response, we proposed model modifications, transitioning the motor case from a two-point to a three-point contact configuration and introducing additional frames beneath the LSD for better stress distribution. These improvements aimed to optimize frame loads, minimize motor case displacement, and enhance the fatigue safety factor, thereby contributing significantly to the advancement of custom high-speed electric vehicle designs.

Key Words: Modeling and Simulation, Fatigue Analysis, Safety Factor, Frame safety, Self-made electric vehicle,

1. Introduction

The growing demand for electric vehicles[(1)] has driven significant advancements in design and engineering. In line with this trend, our study utilizes ANSYS software to tackle crucial challenges encountered in the high-speed operation of a self-made electric vehicle. Our primary focus is on addressing tension-induced issues that arise from the chain drive mechanism. Tension within the chain drive system gives rise to two main problems during vehicle propulsion.

Firstly, the tension-induced rotation of the 2-point-fixed motor case results in undesirable chain slack. Secondly, stress levels exceeding yield limits are observed beneath the LSD (Limited Slip Differential) and motor case frames due to the applied tension. This study is dedicated to systematically analyzing and mitigating these challenges to enhance the performance and reliability of high-speed electric vehicles. Our approach involves determining the maximum chain tension under extreme conditions, identifying realistic boundary conditions, and conducting simulations to assess stress and displacement during actual driving scenarios.

Furthermore, given the cyclic loading experienced by the chain during regular operation, a zero-based force-based fatigue analysis becomes essential to ensure the structural integrity of critical components. To address these challenges, we propose modifications to the existing model, transitioning the motor case from a 2-point to a 3-point contact configuration, and introducing additional frames beneath the LSD for load distribution. Through these enhancements, our goal is to optimize frame loads, mitigate motor case displacement, and improve the fatigue safety factor. This contribution aims to advance the overall design of self-made high-speed electric vehicles.

2. CAE simulation method

In this section, we introduce the shapes of both the old model, where the two main issues introduced in the Introduction part occurred, and the improved new model. Additionally, since setting boundary conditions and load conditions close to reality is essential for obtaining an accurate solution, the content also introduces the specific conditions that were set. Moreover, the section includes details about the main conditions established for conducting fatigue analysis and the analysis process.

2.1 Comparison of old and new models

The biggest difference between the old model and the new model is the number of fixation points of the motor and the presence or absence of the LSD bottom frame.

2.1.1 Old model

The old model has a structure as shown in Fig 1. In the case of the motor case of the old model, it has a two-point contact type, and one of them is not directly connected to the frame but is connected to the frame through a bracket. Additionally, there is no additional frame to support the rear frame under the LSD part.

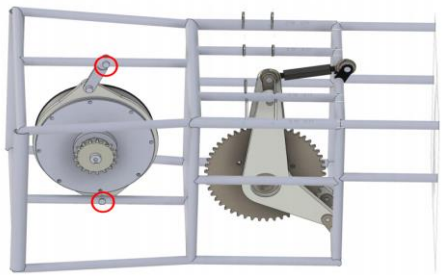

Fig. 1. Old model of vehicle

*발표자(erichwang19@gmail.com), #교신저자(moonhyeonho1026@gmail.com)

2.1.2 New model

The new model has a structure as shown in Fig. 2. With the purpose of minimizing the deformation of the motor case caused by the strong tension generated by the chain, one more fixed contact point was added to the motor case, designing a three-point contact method. Furthermore, to prevent stress concentration in the frame below the LSD, two horizontal frames were additionally designed for load distribution.

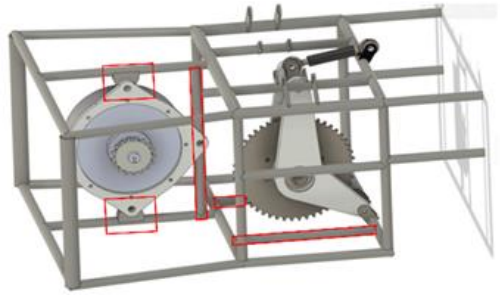

Fig. 2. New model of vehicle

2.2 Materials and mesh convergence

In the process of conducting structural analysis, applying the actual materials used is also an essential step to obtain an accurate solution. This section introduces the materials that were actually used and applied for the analysis of each component, and also discusses the mesh settings that were established for the analysis.

2.2.1 Materials

Various parts are used in vehicles, including the frame, chain sprocket, motor case, LSD, etc. A table that specifies the actual materials used and key physical properties for each part is shown in Table 1. The sprocket and gear, which directly receive the strong tension of the chain, were made of SM45C material, treated with oxide film and high-frequency heat treatment. Additionally, the main frame was made of SM45C, and AL6061-T6 material was used for the Motor case and LSD. The remaining parts were made of structural steel.

Table 1. Component material properties

Component	Material	Main properties
Main frame	SM45C	$E = 200\ [GPa]$ $\sigma_y = 320\ [MPa]$ $\sigma_y = 540\ [MPa]$
Chain sprocket	SM45C (anodized, heat treatment)	Much higher than main frame
Motor case, LSD	AL6061-T6	$E = 70\ [GPa]$ $\sigma_y = 276\ [MPa]$ $\sigma_y = 310\ [MPa]$
Other components	Structural steel	$E = 200\ [GPa]$ $\sigma_y = 250\ [MPa]$ $\sigma_y = 400\ [MPa]$

2.2.2 Mesh convergence

The mesh necessary for the analysis was used as a tetrahedron mesh due to the model's high complexity. Additionally, it was observed that the values of stress according to the mesh began to converge around a mesh size of $20\ [mm]$. Based on this, a mesh size of $10\ [mm]$ was set for areas requiring detailed observation such as the motor case and the bottom frame of the LSD, while a default size was set for other parts to enable faster computation. The form of the mesh set up is as shown in Fig. 3.

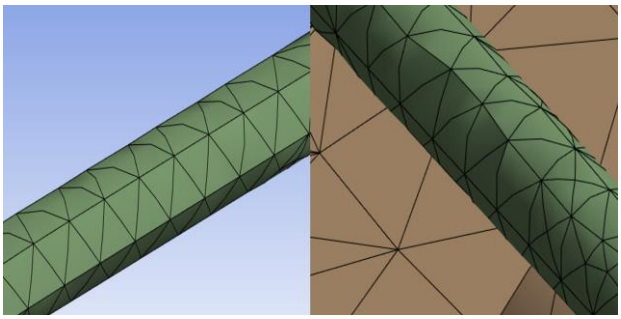

(a) (b)

Fig. 3. Mesh convergence (a) default $45[mm]$, (b) $10[mm]$

2.3 Load condition

The tension in the chain sprocket occurred by rotation of motor is calculated under maximum driving conditions. The vehicle's rated power is $8.8\ [kW]$, with a maximum rpm of $3103\ [rpm]$. Considering a chain sprocket diameter of $69.0\ [mm]$, the calculated chain tension is $784\ [N]$. To account for extreme conditions such as sudden stops and rapid accelerations, multiplication factors[2] were applied, including a usage factor of 1.2, a speed factor of 1.6, an impact factor of 2.0, and a static factor of 1.92. Ultimately, the applied multiplication factors to the initially calculated tension amount to a total factor of 7.37, resulting in a force of $5{,}807\ [N]$ applied to the sprocket for further analysis. Additionally, for the rear top four frames, the reactionary force from the main frame and suspension force are considered[3]. The reactionary force from the main frame is $1393\ [N]$, and the suspension force is $732\ [N]$.

During the load condition, the analysis was performed taking into account two types of contact surfaces. Firstly, for the bolted connections, the connection conditions between bolts and components were treated as bonded. Additionally, for components in contact with each other due to fastening, the connection conditions were set to frictional with a friction coefficient of 0.5. Furthermore, a revolute joint condition was applied between the rod end bearing and the turnbuckle at the rear, allowing rotation around a single axis. Lastly, since each frame is treated as a separate component, the connection points were all set to bonded conditions to accurately reflect the real-world assembly.

2.4 Boundary condition

Fixed support was applied to the vertical frame at the front part of the chassis by selecting the edges. This section is practically connected through seam welding, hence the imposition of such conditions. Additionally, gravitational effects ($1G$) accounting for the vehicle's own weight and acceleration effects ($13.9\ [m/s^2]$) considering the vehicle's inherent rotation were applied. Moreover, for the junctions of the lower and upper arms, given their capability for rotation around the z-axis, a free rotational z condition was applied as a remote displacement condition at eight locations on the rear horizontal frames. The overall schematic representation of the applied forces and boundary conditions is specified in Fig. 4. Analysis condition.

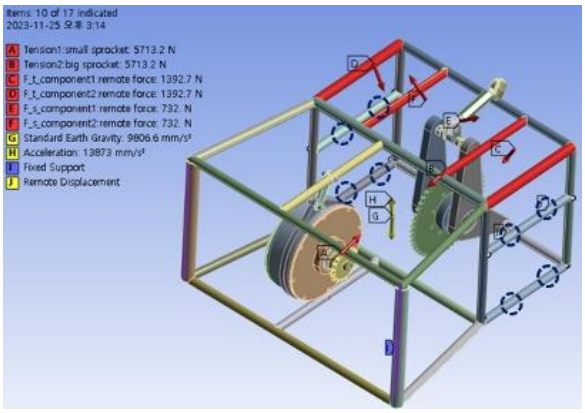

Fig. 4. Analysis condition

2.5 Fatigue analysis

Given the characteristics of rotary machines, it is crucial to meticulously calculate the fatigue life to ensure stable operation during driving. The process of analysis is as follows:

For the main frame of the car, which exceeded the yield stress in the structural analysis (Section 2.1), SM45C steel was used. Since there was no available data for the S-N curve of SM45C, we referred to the graph type of structural steel to draft the S-N curve as shown in Fig. 5. Assuming a maximum lifespan of 10^6 cycles, the fatigue limit σ_e was set using half the value of σ_{ut} provided in Table 1.

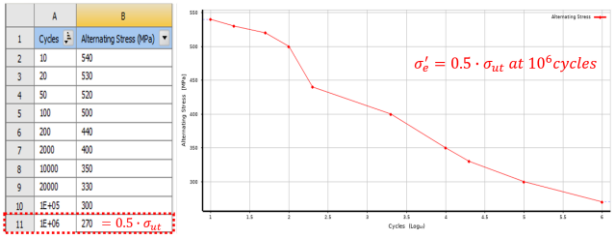

Fig. 5. S-N Curve for SM45C

The chain tension used in the fatigue analysis was not the maximum force as it exceeded the static friction force. Therefore, to utilize a force excluding the static factor, a scale factor of 0.5 was set. Additionally, assuming a zero-base force shape due to the nature of the chain, the fatigue analysis theory was carried out based on Goodman's theory. Furthermore, since the fatigue limit σ_e is a value used in ideal situations, it was conventionally modified by multiplying by 0.5

3. Results and Discussion

By comparing the deformation and equivalent stress results of the problematic model and the improved model for the same force, the performance evaluation of the improved model is conducted. Additionally, considering the expected stress distribution, the increase in the fatigue safety factor for tensile failure at 10^5 cycles in fatigue analysis is assessed. When comparing the improved model with the original model in terms of deformation, stress, and fatigue safety factor, the improved numerical values are summarized in Table 5. Performance of developed model.

3.1 Directional deformation

Firstly, in terms of deformation, the problematic model exhibits larger deformations for the same force compared to the improved model, primarily due to the fewer fixed points in the problematic model. The quantified results are presented in Table 2. Comparison of deformation.

Table 2. Comparison of deformation

Problematic model		Developed model	
Direction	Values [mm]	Direction	Values [mm]
X	13.7	X	1.00
Y	1.94	Y	2.17
Z	3.06	Z	1.00
Total deformation	13.7	Total deformation	2.31

3.2 Equivalent stress

With regard to equivalent stress, it is essential to examine how the stress acting on the frame below the motor and LSD frames has decreased in both the problematic and improved models. In the improved model, the stress under the motor frame has decreased by approximately $390\ [MPa]$ compared to the original model. For the frame under the LSD, the stress has decreased by about $391\ [MPa]$. A detailed comparison of these results is provided in Table 3. Comparison of equivalent stress.

Table 3. Comparison of stress

Problematic model		Developed model	
Part	Stress $[MPa]$	Part	Stress $[MPa]$
Frame under motor case	547	Frame under motor case	157
Frame under LSD	526	Frame under LSD	135

3.3 Fatigue safety factor

As evident from the equivalent stress results, the magnitude of equivalent stress acting on the problematic frame in the improved model has decreased by more than $390\,[MPa]$. Consequently, when conducting an analysis for 10^5 cycles, it is anticipated that the fatigue safety factor in terms of tensile failure will increase. The results of fatigue analysis based on the conditions specified in 2.2. Fatigue analysis are presented in Table 4. Comparison of fatigue safety factor.

Table 4. Comparison of safety factor

Problematic model		Developed model	
Part	SF $[-]$	Part	SF $[-]$
Frame under motor case	0.81	Frame under motor case	3.32
Frame under LSD	0.83	Frame under LSD	3.66

3.4 Discussion

In the old model, the 2-point fixed motor and the absence of frames beneath the LSD resulted in stresses exceeding 500 MPa, surpassing the yield stress of SM45C as shown in Table 1. To address this, the introduction of a 3-point fixed motor and additional frames beneath the LSD significantly reduced the stress by over 70%. Furthermore, deformation decreased from 13mm to 2mm, indicating the elimination of rotation. Based on these findings, fatigue analysis was conducted, revealing that the safety factor of the developed model is four times higher than that of the old model.

This improvement can be attributed to the 3-point fixation, which prevents rotation caused by the motor's torque, and the addition of main frames, which inhibits deformation of the car frame. The reduction in rotation and axial deformation likely diminishes the impact on the chain initially connected to the sprocket and gear, suggesting that more stable driving can be expected.

Table 5. Performance of developed model

Parameter		Degree of improvement
X deformation		12.7 [mm]
Y deformation		0.23 [mm]
Z deformation		2.06 [mm]
Total deformation		11.4 [mm]
Equivalent stress	Frame under motor case	390 $[MPa]$
	Frame under LSD	391 $[MPa]$
Safety factor	Frame under motor case	2.51
	Frame under LSD	2.83

4. Conclusion

Through this project, we successfully demonstrated the significance of a 3-point motor connection and additional frames in enhancing the structural stability of a car. These features effectively prevent rotation and distribute forces. However, this study mainly focused on analyzing a previously damaged old model and developing simulations for the new model. A key limitation of our approach is the lack of real-world testing. We did not verify the stability of the self-made vehicle through actual driving, which may lead to differences between our simulated results and real-world performance.

In light of these findings, our next step involves rebuilding and testing the developed model in real-world conditions. We aim to affirm the structural stability of the self-made vehicle during operation, bridging the gap between theoretical simulations and practical application.

감사의 글

This work was supported by Linc 3.0 Fund of Han-dong University.

참고문헌

1. The Electric Vehicle World Sales Database, https://www.ev-volumes.com/country/total-world-plug-in-vehicle-volumes/
2. Misumi, https://kr.misumi-ec.com/tech-info/categories/technical_data/td03/a0020.html?bid=bid_kr_ec_43766_192
3. Kook, J.H., 2023, *Simulation-based Light Weight Design of A Self-made Electric Vehicle Frame*, Bachelor's Thesis, Handong Global University